

The effect of ultrafine kaolinite aggregation on the performance of quartz cationic flotation

Marta Duarte da Fonseca Albuquerque^{1,2}, Danielle Andrade Pimentel^{1,2},
Alexandro Uliana², Marisa Bezerra de Mello Monte^{1,2} 

¹Centro de Tecnologia Mineral. Av. Pedro Calmon, 900, Cidade Universitária, 21941-908, Rio de Janeiro, RJ, Brasil.

²Samarco Mineração S.A., Coordenação de Desenvolvimento de Processos, Rodovia MG-129, km 117.5, 35420-000, Distrito de Bento Rodrigues, Mariana, MG, Brasil.

e-mail: alexandro.uliana@samarco.com; mmonte@cetem.gov.br; mduarte@cetem.gov.br; pimentel.danielle@gmail.com

ABSTRACT

This work presents a study on the interference of kaolinite particles, smaller than 10 μm , in the performance of the cationic flotation of quartz. The surface properties control the effects of heteroaggregation and provide the creation of a coverage of these ultrafine on the coarser particle surfaces (slime coating), which makes it difficult for the collectors to adsorb and/or contact the air bubbles. The flotation experiments revealed that the etheramine collector used is capable of recovering 76.9% of ultrafine kaolinite in the absence of coarse quartz particles. On the other hand, the flotation results carried out with the binary mixture (quartz $-150 + 45 \mu\text{m}$ and kaolinite ultrafines $-6 \mu\text{m}$) and in the presence of the same reagent system showed that kaolinite floats together with quartz depending on the content of ultrafines in the suspension. Micrographs from MEV/EDS showed that a heterocoagulation between coarse quartz particles and kaolinite ultrafine with a formation of hydrophobic agglomerates can be recovered in the flotation.

Keywords: Ultrafines; Kaolinite; Quartz; Flotation.

1. INTRODUCTION

Slime coating is related to fine gangue minerals generated due to the fine grind or the clayey nature of the ore. These fine particles exert detrimental effects on the flotation process due to the: i) adhesion of gangue slime to coarse particle surface, ii) slimes are bound to the value mineral surfaces through chemical reactions; iii) deposition of plate-like agglomerates on the mineral surface, during ore comminution; iv) the increasing of the reagent consumption and pulp viscosity; v) prevention of the value mineral from direct contact with collectors and/or air bubbles [1]. In most cases, the slimes are composed of kaolinite, montmorillonite, illite, serpentine, quartz, and dolomite and their interference on the performance of flotation is usually attributed to the 5 μm particles or lesser.

The classical Derjaguin-Landau-Verwey-Overbeek (DLVO) has been widely used to understand the particle/particle adhesion phenomena, from the point of view of chemical interactions. OATS *et al.* [2] calculated the interaction forces between coal and clay particles using DLVO theory based on the Lifshitz approach. Their results showed that the van der Waals attraction was strong enough to overcome the electrical double – layer repulsion, resulting in a net attraction between these particles at a close separation distance.

MA *et al.* [3] reported that slimes were a type of the chemical precipitation that could occur depending on the chemistry conditions of the ore pulp. In quartz cationic flotation, the presence of ultrafine particles negatively influences the performance of the iron ore concentration process, depending on the origin of the ore, some have a large number of finely disseminated minerals (such as kaolinite, gibbsite and goethite, among others), which are potential sources of fines generation.

The surface properties (wettability, flotability, zeta potential, and surface free energy) control the effects of aggregation and influence the creation of a coating of these slimes on the coarser particles, which makes it difficult for collectors to adsorb and/or contact with the air bubbles. A small particle mass also causes low momentum with less probability of collision with a bubble and adhesion to it [4]. A high specific surface, combined with a higher surface energy activity of these ultrafine particles, can also result in excessive consumption of reagents, less selectivity in the adsorption of collectors, and rigidity in the froth. The advances in the quantitative measurements

of interaction forces of particle-particle, bubble-particle, and particle-reagent are discussed by XIE *et al.* [5]. They reported that nanobubbles or hydrophobic nanoparticles could be adhering to hydrophobic domains of fine particles and improving the bubble-particle attachment. AFM force mapping provides valuable information on the size and distribution of nanoscopic hydrophobic domains on the mineral surfaces.

The main composition of the ultrafine particles in the Iron Quadrangle of the State of Minas Gerais would be 70% hematite, 25% quartz, and 5% kaolinite [6, 7]. The behavior of kaolinite in the cationic flotation of quartz has been explained based on considerations of its crystalline structure. The different properties of surface charge between the edges and faces of kaolinite make the behavior of these particles in flotation, conducted with cationic collectors and in the presence of gelatinized starch, very different when compared to quartz and iron oxides. Its adsorption sites are found on the octahedral sheet and on the side faces of the crystal, which can be positive $AlOH_2^+$ or negative AlO^- , depending on the pH of the medium, and on the surface of the kaolinite silicon sheet the generation of charge does not depend on the suspension pH value.

The weak affinity between the starch molecules and the kaolinite surface, in the most alkaline range of pH, was observed by MA and BRUCKARD [8], from adsorption tests conducted with kaolinite fines (BET area = 10.7 m²/g) conditioned in starch solutions, for a wide range of evaluated concentrations. Only when the pH values decrease from 10.5 to 7, a reduction in the value of kaolinite's negative charge observed, favoring the adsorption of ionic starch molecules. Flotation experiments of a synthetic mixture of hematite and kaolinite, carried out in the presence of starch, as a depressant and etheramine, as a collector, showed the recoveries of kaolinite and hematite of 43% and 7%, respectively [9]. According to the authors, the adsorption of etheramine would occur at the sites of the SiO₄ faces of kaolinite.

In this work, the flotation studies with a synthetic mixture of natural minerals, quartz (fraction < 150 μm) and ultrafine kaolinite (fraction < 6 μm) were carried out, using the conventional system of reagents for the reverse flotation of itabirite ore. The interference of ultrafine particles (smaller than 10 μm) in the performance of cationic quartz flotation was the focus of this research besides the phenomenon of covering quartz particles with ultrafine kaolinite particles. Measurement techniques to characterize the phenomenon of heterocoagulation were carried out in order to contribute to the understanding of the interaction between these particles and the formation of hydrophobic agglomerates. Theoretical calculations applying the DLVO theory were also performed to evaluate the interaction between these ultrafines (<10 μm) and the coarser fractions, which could explain the increase in the grade of silica and aluminum in Brazilian iron ore concentrates.

2. MATERIAL AND METHODS

2.1. Materials

The quartz samples of high purity used in this study were purchased from Minas Gerais State and kaolinite from Pará State in Brazil. The chemical composition of the samples was determined using a X-ray fluorescence (XRF) spectrometer (model AXIOS, from Panalytical) and an inductively coupled plasma optical emission spectrometer (ICP-OES) (model Ultima 2, with radial view, Horiba Jobin Yvon, Longjumeau, France). The Table 1 summarize the quantitative determination of the elements and compounds obtained for the samples. The results indicate that the major components are Fe with minor to trace amounts of Ti, Cr, Al, Si, Ca, and Mn for the kaolinite sample. For the quartz samples, the main component Si (46.32%) minor amounts of Fe (0.11%) and Ca (0.22%).

The samples were carefully ground, avoiding fines production and contamination, using an agate mortar and pestle. The particles size of the samples adjusted between -150 + 45 μm and -6 μm, respectively.

All the reagents used were of analytical grade. Corn starch and etheramine were obtained from commercial companies, Flokit 415 and Clariant, respectively. For pH adjustment, dilute solutions of HCl and NaOH were employed. Ultrapure water produced by Milli-Q® Direct 8 purification System was used for all experiments. The water conductivity was 0.05 μS/cm.

2.2. Methods

The particle size distribution determination tests were performed using a laser granulometer Malvern, model Mastersizer 2000 SM.

2.2.1. Particle size distribution tests

Figure 1(a) shows the results for particle size distribution of coarse quartz sample used in the micro-flotation. Thus, more than 80% the particles of sample were less than 150 μm, with the average particle size of 104 μm (d50). The particle size distribution curve of kaolinite sample is presented in the Figure 1(b). It was observed that 80% of the kaolinite particles were less than 8.4 μm. The curve from Figure 1(c) shows the finer quartz sample with average particle size of 6 μm (d50).

Table 1: X-ray fluorescence (XRF) and inductively coupled plasma optical emission spectroscopy (ICP-OES) of kaolinite and quartz samples.

SAMPLES	ELEMENT/OR COMPOUNDS	CHEMICAL ANALYSIS (%)
Kaolinite	Fe	0.3
	TiO ₂	0.835
	Cr	0.21
	SiO ₂	44.8
	Al ₂ O ₃	38.78
	Mn	–
	MgO	0.310
	CaO	<0.10
	PPC	14,4
Quartz	Si	46.32
	Ca	0.22
	Fe	0.11
	Cr	<0.10
	Al	<0.10
	K	–
	Mn	–
	Mg	–

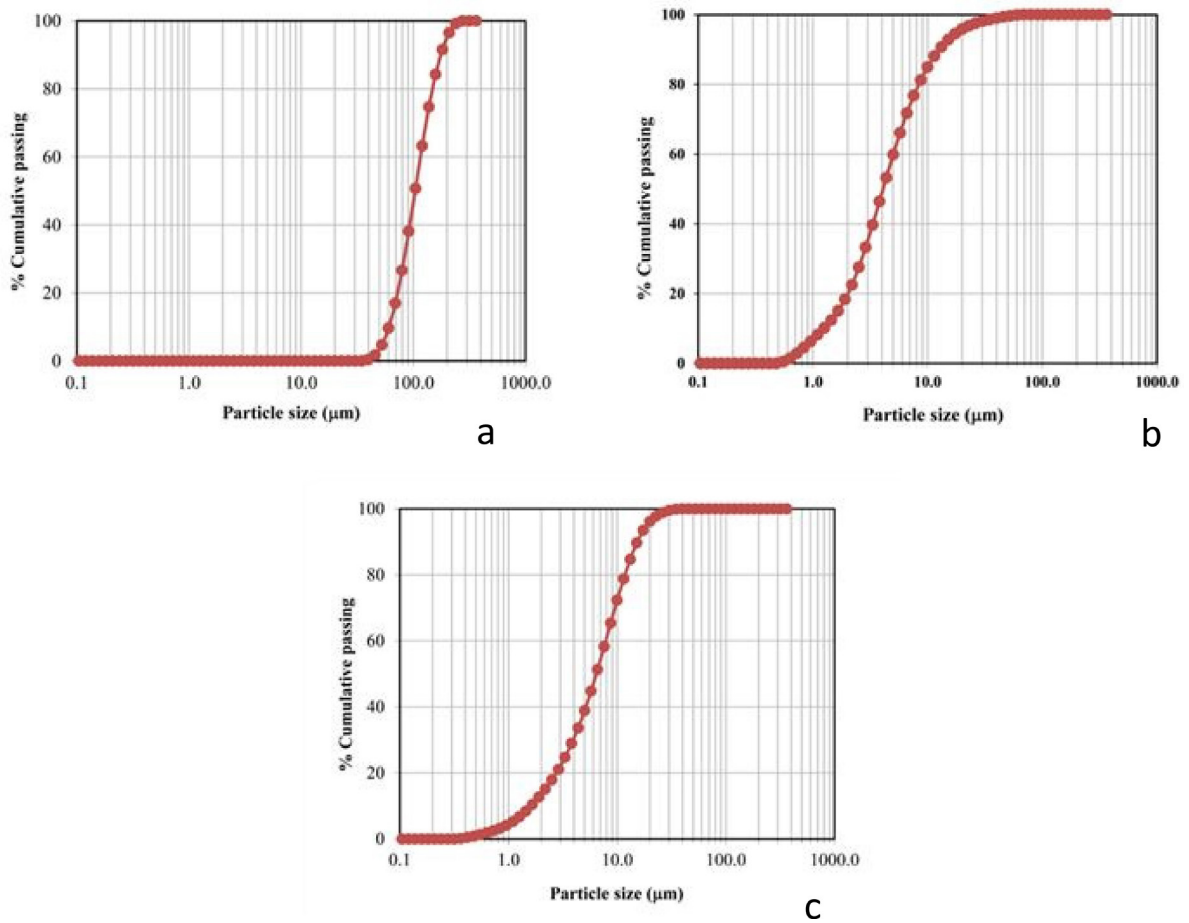


Figure 1: (a) Particle size distribution curve of the coarse quartz sample. (b) Particle size distribution curve of the kaolinite sample. (c) Particle size distribution curve of the finer quartz sample.

2.2.2. Micro-flotation experiments

The flotation tests of the isolated minerals and, also, in the presence of the binary mixture, were performed in a 300 ml Partridge-Smith tube. In these tests, the depressant reagent used was cassava starch, was used as a depressant, which was previously gelatinized with NaOH solution (1M) resulting in a concentrated suspension of 50% w/v (in a mass ratio between starch and soda of 5 to 1). In addition, stock solutions of the ethermonoamine and etherdiamine were used as collectors which were prepared at a concentration equal to 1% w/v. HCl and NaOH solutions were used as pH regulators. The experiments were carried out with 2 g of mineral sample, using distilled water. Afterwards, a mixture of the collectors, ethermonoamine and etherdiamine, at a concentration of 50 mg/L was added, and the conditioning was another 1 min. The cell volume was made up water and the flotation time was to 4 min. The air flow rate used was 15 mL/min. The products (floated and sunk) were filtered, dried, and weighed.

The floatability of the minerals was evaluated by calculating the percentage of floated material (Equation 1). In the experiments carried out in the presence of the mineral mixture, the floated material was separated with the aid of a sieve with a 38 μm aperture. The same equation was used to calculate the floated percentage of the fine minerals recovered in the froth, it was considered only the mass obtained in the fraction less than 38 μm .

$$F = \frac{m_o}{m_o + m_u} \times 100 \quad (1)$$

where F is the floatability or percentage floated, m_o is the solid mass of the floated portion and m_u is the solid mass of the sunken portion. The variation of the floatability values obtained was $\pm 3\%$.

2.2.3. Analysis of the DLVO interaction energy

The interactions between kaolinite and quartz in aqueous solution can be considered include the van der Waals force and the electrostatic double layer force. From the DLVO theory (Equation 2), which depends on van der Waals (Equation 3) and electrostatic (Equation 4) forces, it was possible to estimate the interaction energy curves for quartz and kaolinite [10–14].

$$\Delta G_{Tot} = \Delta G_{vdW} + \Delta G_{ELE} \quad (2)$$

$$\Delta G_{vdW} = -\frac{A_{132}a_1a_2}{6(a_1 + a_2)H_0} \quad (3)$$

$$G_{ELE} = 32\pi\epsilon_a \left[\frac{a_1a_2}{2(a_1 + a_2)} \right] \left(\frac{\kappa_b T}{Z_e} \right)^2 \tanh\left(\frac{Ze\gamma_1}{4\kappa_b T} \right) \tanh\left(\frac{Ze\gamma_2}{4\kappa_b T} \right) e^{-\kappa H_0} \quad (4)$$

Where A_{132} is the effective Hamaker constant of materials 1 and 2 in medium 3 (J), a is the particle radius (m), H_0 is the minimum separation distance between particles (m); ϵ_a is the product of the vacuum permittivity and the dielectric constant of the medium ($8.854 \times 10^{-12} \text{ F.m}^{-1}$), k_b is the Boltzmann constant t, $1.3806 \times 10^{-23} \text{ J.K}^{-1}$, T is the temperature (K), Z is the valence of the ion, e is the charge of the electron ($1.602 \times 10^{-19} \text{ C}$), γ is the zeta potential of particles 1 and 2 (V), and k is the Debye-Huckel length (m^{-1}).

The individual Hamaker constant can be calculated from Equation 5 and the effective Hamaker constant, for a system of materials 1 and 2 in a medium 3, can be calculated from Equation 6 [15].

Table 2: Individual Hamaker constants and surface potential values for quartz and kaolinite.

SURFACE	A (10^{-20} J)	SURFACE POTENTIAL (mV)
Quartz	8.8	- 21.0
Kaolinite	6.8	- 45.0

$$A_{11} = \frac{3}{4} \kappa_b T \frac{(\epsilon - 1)^2}{(\epsilon + 1)^2} + \frac{3h\nu_{UV}(n^2 - 1)^2}{16\sqrt{2}(n^2 + 1)^{3/2}} \quad (5)$$

$$A_{132} = \left(\sqrt{A_{11}} - \sqrt{A_{33}}\right)\left(\sqrt{A_{22}} - \sqrt{A_{33}}\right) \quad (6)$$

where k_b is the boltzmann constant, T the temperature, ϵ the dielectric constant of the medium, for water 79, h the Planck constant, ν_{UV} is the main frequency of electronic absorption in the ultraviolet region and n is the refractive index of the material.

Interaction energies between coarse quartz, ultrafine kaolinite, and ultrafine quartz particles at pH 10.5 were obtained. Table 2 shows the individual Hamaker constant and the surface potential (constant ionic strength of 1×10^{-4} M KNO_3) used in this work for quartz and kaolinite, respectively [16-17].

2.2.4. Scanning Electron Microscopy (SEM)/Energy-Dispersive X-Ray Spectroscopy (EDS)

The morphological analyses of the mineral samples performed using the scanning electron microscopy, operated in the backscattered electron visualization mode, and the samples were previously coated with a thin layer of silver by evaporation in the BAL-TEC SCD 005 Sputter Coater metallizer. For this analysis, a HITACHI microscope model TM3030 Plus was used with a high vacuum and electron acceleration voltage of 15 kV. To identify the elements present in the samples, energy dispersive X-ray spectroscopy was also used. The equipment used in this case was the Bruker Quantax 70, which is coupled to the SEM.

In this experiment, a binary mixture was used between minerals containing quartz particles and ultrafine kaolinite particles, where the contained of ultrafines was 10%. This combination was placed inside the bottom of the Partridge Smith flotation cell and then added to water at pH 10.5 and the magnetic stirrer was activated. The gelatinized cassava starch (300 mg/L) was added, carrying out a conditioning for 5 minutes. The collector mixture was added and conditioning was carried out for another 1 minute Then more water at pH 10.5 was added to make up the volume to 50 ml. After 4 minutes of stirring, a drop of the suspension was collected and placed on a slide. The slides were kept in a desiccator for later analysis.

3. RESULTS AND DISCUSSION

3.1. Microflotation test with artificial mixture

The aim of these experiments was to investigate the interaction between fine kaolinite and coarse quartz particles in the cationic reverse flotation of iron ore process. The result for quartz flotation is shown in Figure 2 besides the influence of the ultrafine kaolinite (0, 5, and 10 %) additions on its floatability. It can be seen from Figure 2 in this graph that the increase in the percentage of ultrafines in the suspension provided an increase in the floatability of kaolinite, whose recovery went from 30% (5% of ultrafines) to 47.3% in the presence of 10% of these ultrafines.

The mixture of collectors promoted the flotation of kaolinite in 76.9%, compared to the flotation performed only with the diamine collector, which presented floatability equal to 57.7% for this mineral, explained by the fact that the specific surface area of kaolinite ultrafine is high and also by the interaction of the kaolinite

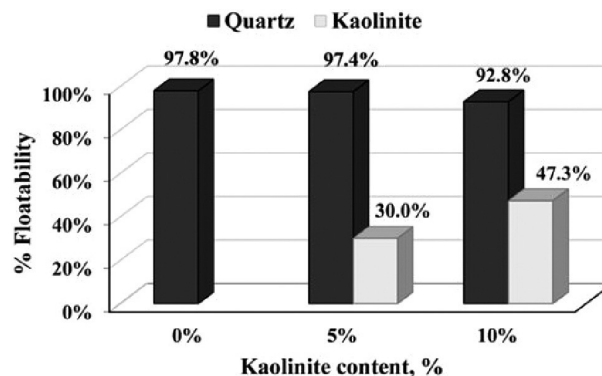


Figure 2: Effect of ultrafine kaolinite ultrafine addition on quartz floatability.

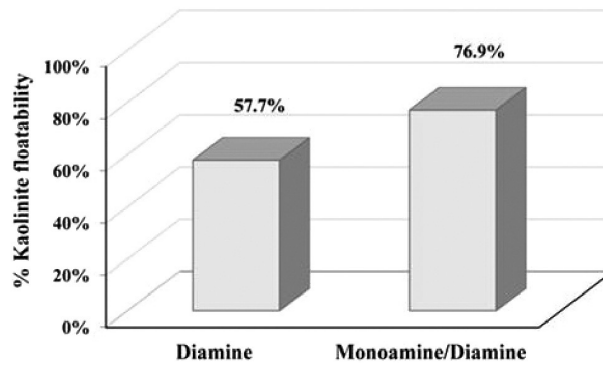


Figure 3: Kaolinite floatability in the presence of starch and in different type of collectors.

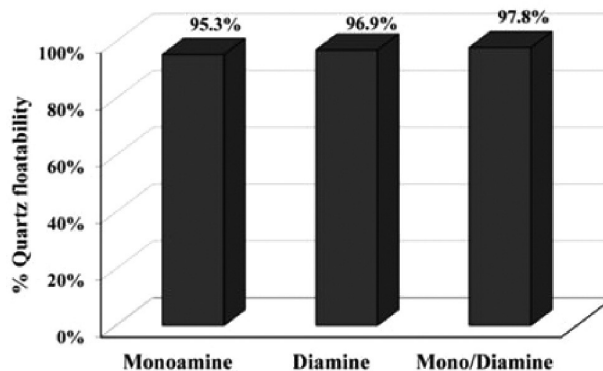


Figure 4: Quartz floatability in the presence of starch and in different collectors.

surface with the amines used (Figure 3). Figure 4 shows quartz floatability in the presence of starch and different collectors. These quartz floatability in different collectors is not affected.

3.2. Interaction energy evaluation

Based on the van der Waals and electrical interaction energies as a function of the distance between; coarse quartz – ultrafine kaolinite; ultrafine kaolinite – ultrafine kaolinite; coarse quartz – ultrafine quartz, and ultrafine quartz – ultrafine quartz, in the absence of flotation chemicals, at pH = 10.5 were calculated and illustrated in Figure 5 (a) and (b) and Figure 6 (a) and (b), respectively. The DLVO energy profiles exhibit an evident repulsion between ultrafine kaolinite and coarse quartz particles, ultrafine kaolinite and ultrafine kaolinite, in the absence of reagents (Figure 5 (a) and (b)). Figure 6 (a) and (b) also shows repulsive forces between coarse quartz and ultrafine quartz and ultrafine quartz particles, respectively. These results agree those obtained by LI *et al.* [18], who obtained repulsive forces at pH 11 for the interaction between the aluminum-oxygen surface of kaolinite and silicon-oxygen surface of kaolinite/quartz particles.

The attractive surface forces can induce and strengthen the aggregation of hydrophilic kaolinite on quartz minerals, while the repulsive surface forces tend to prevent the aggregation [5]. Without the flotation chemicals, the hydrophobic attraction was not present to facilitate the aggregation among them. However, it can also be noted that there an energy barrier between the coarse quartz and ultrafine kaolinite of 1.53×10^{-17} J that has to be overcome in order to induce the coagulation for a separation distance of 0.53 nm. Hydrophilic ultrafine kaolinite is capable to be entrained in the water film confined between air bubbles and the coagulation phenomena could reduce the entrainment of hydrophilic fines.

3.3. Scanning Electron Microscopy (SEM)/Energy-Dispersive X-Ray Spectroscopy (EDS)

SEM image and EDS spectrum obtained for the binary mixture of coarse quartz and ultrafine kaolinite is shown in Figure 7. Figure 8 shows the SEM-EDS map for the binary mixture. The image from Figure 7 revealed that the kaolinite ultrafines are covering the quartz surface, that is, there is a heterocoagulation between the particles with the formation of hydrophobic agglomerates.

Figure 9 presents the SEM micrographs and the EDS spectra obtained for the coarse quartz and ultrafine kaolinite, separately. The EDS spectrum shown in Figure 9 (b) revealed that the elements present are silicon,

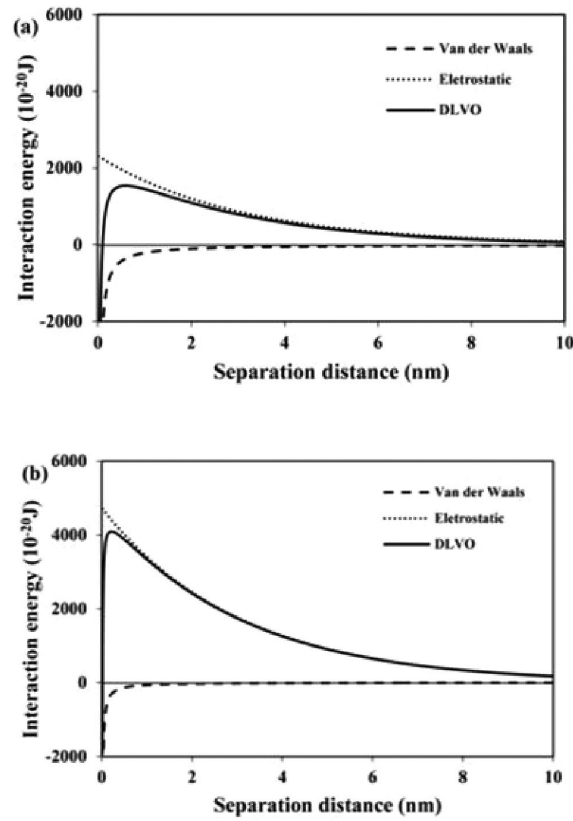


Figure 5: Calculated DLVO interaction between: (a) coarse quartz and ultrafine kaolinite and (b) ultrafine kaolinite particles as a function of the separation distance and at pH 10.5.

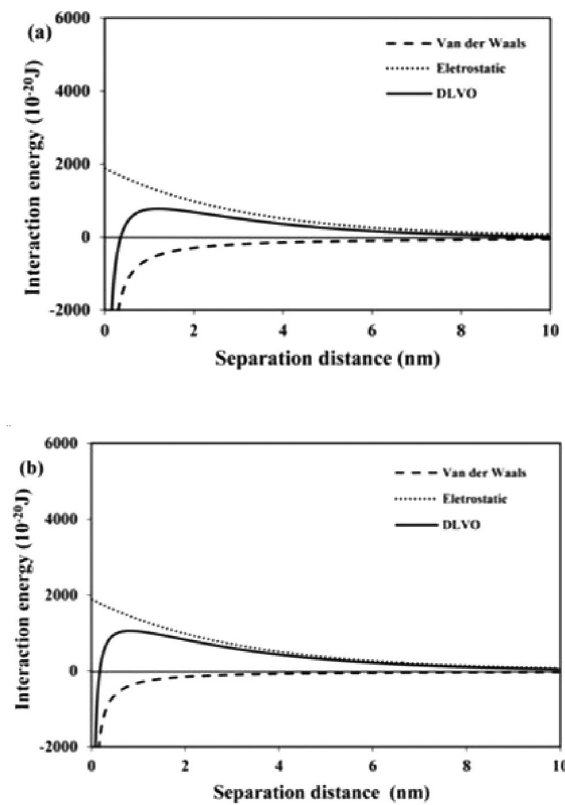


Figure 6: Calculated DLVO interaction between: (a) coarse quartz and ultrafine quartz and (b) ultrafine quartz particles as a function of the separation distance and at pH 10.5.

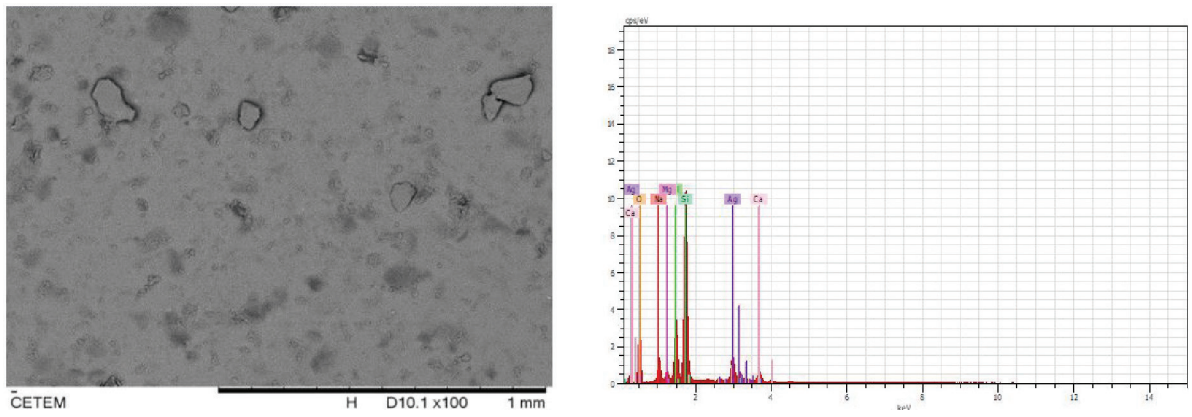


Figure 7: SEM image and EDS spectra of the binary mixture of coarse quartz and fine kaolinite.

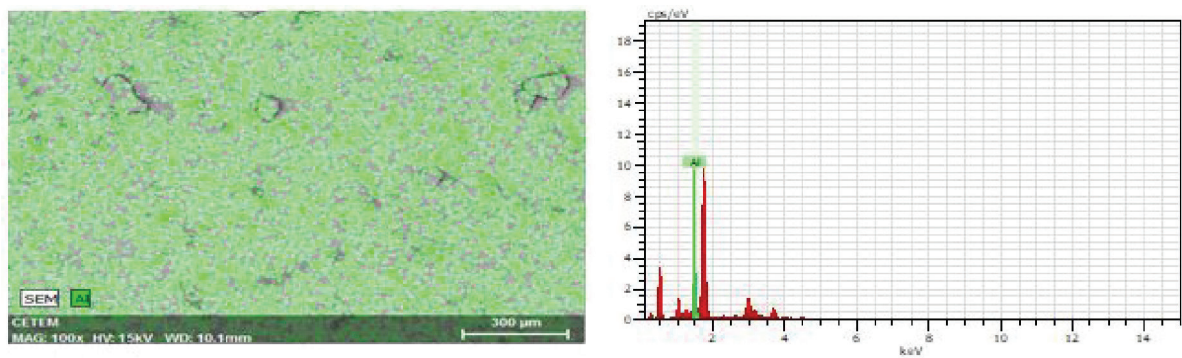


Figure 8: SEM-EDS map.

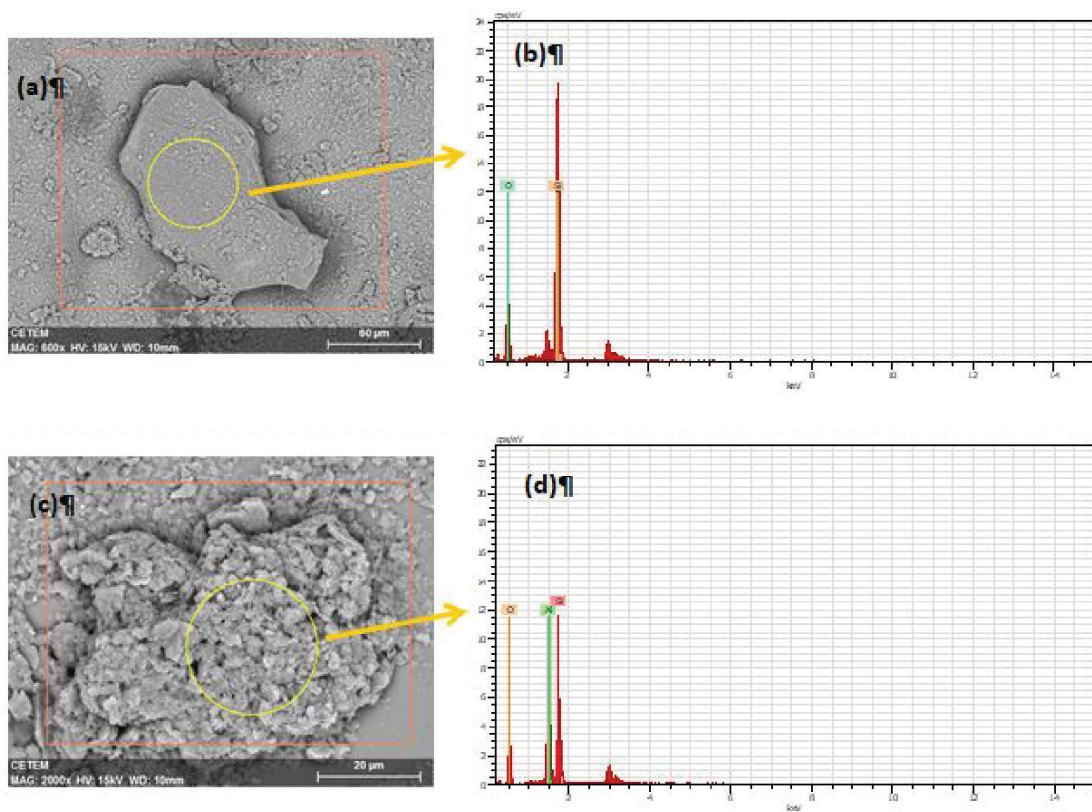


Figure 9: SEM image and EDS spectra: (a) and (b) coarse quartz; (c) and (d) kaolinite ultrafines, respectively.

oxygen, and aluminum (not highlighted) showing that the quartz covered by kaolinite particles. In the case of the EDS spectra of Figure 9 (d), which were carried out with only kaolinite, showing the following elements: aluminum, oxygen, and silicon.

4. CONCLUSIONS

The results obtained from this study indicate that the presence of the kaolinite ultrafines has a significant on the separation of quartz from iron ore in the cationic flotation system. It was observed that the quartz recovery decreased with the increase of kaolinite content in the flotation pulp.

In this study, quartz and kaolinite interaction decreased due to the increase of the electrostatic repulsive forces at pH 10. The results presented here indicate that the addition of reagents changes the surface chemistry, allowing particles to interact even at high pH values where both minerals exhibit negative zeta potential values. In the presence of amines, the hydrophobic attraction was present to facilitate the hydrophobic aggregation among them. The SEM analysis of the binary mixture in the presence of a reagent system show that there are silica particles are dispersed as well as being attached to kaolinite. Although, only a few particles (or aggregates) are shown in the SEM image obtained for the binary mixture (coarse quartz and fine kaolinite), there is good evidence for kaolinite misreporting to the frother via aggregation with quartz.

5. BIBLIOGRAPHY

- [1] YU, Y., MA, L., CAO, M., *et al.*, “Slime coatings in froth flotation: a review”, *Minerals Engineering*, v. 114, pp. 26–36, Dec. 2017. doi: <http://dx.doi.org/10.1016/j.mineng.2017.09.002>.
- [2] OATS, W.J., OZDEMIR, O., NGUYEN, A.V., “Effect of mechanical and chemical clay removals by hydrocyclone and dispersant on coal flotation”, *Minerals Engineering*, v. 23, n. 5, pp. 413–419, Apr. 2010. doi: <http://dx.doi.org/10.1016/j.mineng.2009.12.002>.
- [3] MA, X., MARQUES, M., GONTIJO, C., “Comparative studies of reverse cationic/anionic flotation of Vale iron ore”, *International Journal of Mineral Processing*, v. 100, n. 3-4, pp. 179–183, Jul. 2011. doi: <http://dx.doi.org/10.1016/j.minpro.2011.07.001>.
- [4] ARAUJO, V.A., LIMA, N., AZEVEDO, A., *et al.*, “Column reverse rougher flotation of iron bearing fine tailings assisted by HIC and a new cationic collector”, *Minerals Engineering*, v. 156, n. 1, pp. 106531, Sep. 2020. doi: <http://dx.doi.org/10.1016/j.mineng.2020.106531>.
- [5] XIE, L., WANG, J., LU, Q., *et al.*, “Surface interaction mechanisms in mineral flotation: fundamentals, measurements, and perspectives”, *Advances in Colloid and Interface Science*, v. 295, pp. 102491, Jul. 2021. doi: <http://dx.doi.org/10.1016/j.cis.2021.102491>.
- [6] RODRIGUES, O.M.S., PERES, A.E.C., MARTINS, A.H., *et al.*, “Kaolinite and hematite flotation separation using etheramine and ammonium quaternary salts”, *Minerals Engineering*, v. 40, pp. 12–15, Jan. 2013. doi: <http://dx.doi.org/10.1016/j.mineng.2012.09.019>.
- [7] LIMA, N.P., SILVA, K., SOUZA, T., *et al.*, “The characteristics of iron ore slime and their influence on the flotation process”, *Minerals (Basel)*, v. 10, n. 8, pp. 675, Jul. 2020. doi: <http://dx.doi.org/10.3390/min10080675>.
- [8] MA, X., BRUCKARD, W.J., “The effect of pH and ionic strength on starch–kaolinite interactions”, *International Journal of Mineral Processing*, v. 94, n. 3-4, pp. 111–114, Apr. 2010. doi: <http://dx.doi.org/10.1016/j.minpro.2010.01.004>.
- [9] SILVA, K., FILIPPOV, L.O., PIÇARRA, A., *et al.*, “New perspectives in iron ore flotation: Use of collector reagents without depressants in reverse cationic flotation of quartz”, *Minerals Engineering*, v. 170, pp. 107004, Aug. 2021. doi: <http://dx.doi.org/10.1016/j.mineng.2021.107004>.
- [10] VILINSKA, A., RAO, H.K., “Surface Thermodynamics and extended DLVO Theory of acidithiobacillus ferrooxidans cells adhesion on pyrite and chalcopyrite”, *The Open Colloid Science Journal*, v. 2, n. 1, pp. 1–14, 2009. doi: <http://dx.doi.org/10.2174/1876530000902010001>.
- [11] BOTERO, A.E., TOREM, M.L., DE MESQUITA, L.M.S., “Surface chemistry fundamentals of biosorption of *Rhodococcus opacus* and its effect in calcite and magnesite flotation”, *Minerals Engineering*, v. 21, n. 1, pp. 83–92, Jan. 2008. doi: <http://dx.doi.org/10.1016/j.mineng.2007.08.019>.
- [12] YAO, J., HAN, H., HOU, Y., *et al.*, “A method of calculating the interaction energy between particles in minerals flotation.”, *Mathematical Problems in Engineering*, v. 2016, pp. 1–13, 2016. doi: <http://dx.doi.org/10.1155/2016/8430745>.

- [13] YIN, W., WANG, J., “Effects of particle size and particle interactions on scheelite flotation”, *Transactions of Nonferrous Metals Society of China*, v. 24, n. 11, pp. 3682–3687, Nov. 2014. doi: [http://dx.doi.org/10.1016/S1003-6326\(14\)63515-9](http://dx.doi.org/10.1016/S1003-6326(14)63515-9).
- [14] ISRAELACHVILI, J.N., *Intermolecular and surface forces*, 3rd ed., San Diego, Academic Press, 2011.
- [15] MÉDOUT-MARÈRE, V., “A Simple experimental way of measuring the hamaker constant A_{11} of divided solids by immersion calorimetry in apolar liquids”, *Journal of Colloid and Interface Science*, v. 228, n. 2, pp. 434–437, Aug. 2000. <http://dx.doi.org/10.1006/jcis.2000.6984>.
- [16] LINS, F.F., MIDDEA, A., ADAMIAN, R., “Processing of hydrophobic minerals and fine coal”, In: *Proceedings of the First UBC-McGill Bi-Annual International Symposium on Fundamentals of Mineral Processing*, pp. 61, Vancouver, B.C., Canada, 1995.
- [17] MARINS, T.F., “Avaliação de eletrólitos indiferentes na determinação do potencial zeta de minerais”, Trabalho de Conclusão de Curso, Universidade Federal de Ouro Preto, Ouro Preto, 2017.
- [18] LI, Y., XIA, W., WEN, B., *et al.*, “Filtration and dewatering of the mixture of quartz and kaolinite in different proportions”, *Journal of Colloid and Interface Science*, v. 555, pp. 731–739, Nov. 2019. doi: <http://dx.doi.org/10.1016/j.jcis.2019.08.031>.